# Proposal for graphene-based coherent buffers and memories

L. Zhao[1,2] and S. F. Yelin[1,3]
[1]*Department of Physics, University of Connecticut, Storrs, Connecticut 06269, USA*
[2]*Department of Physics, Tsinghua University, Beijing 100084, People's Republic of China*
[3]*ITAMP, Harvard-Smithsonian Center for Astrophysics, Cambridge, Massachusetts 02138, USA*
(Received 23 January 2010; published 22 March 2010)

We theoretically show that it is possible to coherently control the group velocity of graphene quasiparticles based on tunable electric field effects in both single layer and bilayer graphene *p-n-p* waveguides, whereby graphene-based coherent buffers and memories could be proposed. We also find that the essential mechanism for the coherent buffering and trapping of quasiparticles can be attributed to interband tunneling through *p-n* interfaces.

DOI: 10.1103/PhysRevB.81.115441 PACS number(s): 73.21.−b, 42.82.Et, 72.80.Vp, 81.05.U−

Graphene systems including both single layer graphene (SLG) and bilayer graphene (BLG) are now actively explored.[1–3] In SLG, its quasiparticles at low energy are *massless* Dirac fermions with a linear (relativistic) spectrum. Besides, SLG quasiparticles have anomalous quantum Hall effects[4,5] and Klein tunneling.[6] In contrast to SLG, BLG quasiparticles at low energy are *massive* Dirac fermions with a parabolic (nonrelativistic) spectrum. And, they show unconventional quantum Hall effects[7] and BLG chiral tunneling.[6] Moreover, the band gaps of BLG can be tuned by external electric field effects.[8,9]

To realize practical graphene-based electronic processors, quasiparticle trapping is an important prerequisite. Inspired by electron trapping in semiconductor-based quantum dots,[10] a straightforward solution to achieve quasiparticle trapping is using SLG and BLG quantum dots.[11–14] Another intuitive method is using magnetic fields to control the motion of quasiparticles.[15–19] On the other hand, it is well known that SLG quasiparticles indicate some photon-like properties, such as electron beam supercollimation,[20] subwavelength graphene nanodevices,[21] and focusing through SLG *p-n* interfaces.[22] Recently, photon buffering and trapping in left-handed heterostructures (LHHs), called "trapped rainbow" storage, has been proposed.[23] Considering the similarities between SLG quasiparticles and photons,[22] SLG *p-n-p* waveguides can be directly analogous to the photonic LHH,[24,25] whereby SLG quasiparticles might be coherently buffered and stopped. This effect may provide an alternative method to buffer and trap SLG quasiparticles. However, coherent trapping of BLG quasiparticles is also a nontrivial problem. Due to the remarkable differences between SLG and BLG mentioned above, it is still an open question whether BLG quasiparticles could be coherently manipulated in a similar manner.

In this paper, we thus systematically examine the possibility of coherently controlling group velocity of both SLG and BLG quasiparticles in electric-field induced *p-n-p* waveguides in *bulk* graphene. (Experimentally, large-area and high-quality bulk graphene sheets have been synthesized and transferred to $SiO_2/Si$ substrates.[26,27] Tunable local electrostatic gates of nanometer scale can be fabricated to modulate the charge density in the graphene sheets, thus producing the waveguide configurations of graphene *p-n-p* junctions.[28,29]) As an interesting result, we find that not only SLG but also BLG quasiparticles can be coherently buffered and trapped. This result clearly indicates that quasiparticle buffering and trapping in graphene *p-n-p* waveguides are irrelevant to the photon-like linear (relativistic) spectrum, and the essential mechanism should be attributed to *interband tunneling* through the *p-n* interfaces.

In a SLG *p-n-p* waveguide [Figs. 1(a)–1(c)], also called a graphene quantum well in Ref. 30, the quasiparticle dynamics is governed by the Dirac equation,[2,3,30]

$$[-i\hbar v_F(\boldsymbol{\sigma}\cdot\boldsymbol{\nabla})+V(x,y)]\psi=E\psi, \tag{1}$$

where $v_F\approx 10^6$ m/s is the Fermi velocity, $\boldsymbol{\sigma}=(\sigma_x,\sigma_y)$ are the Pauli matrices, and $E$ is the eigenenergy. The electrostatic potential $V(x,y)$ is given by

$$V(x,y)=\begin{cases}0 & 0\le x\le w,\\ V_0 & \text{otherwise},\end{cases} \tag{2}$$

where $w$ is the width of region *I*. Because a unit cell of the graphene honeycomb lattice contains two sublattices A and B, the eigenstates $\psi$ can be expressed by two-component

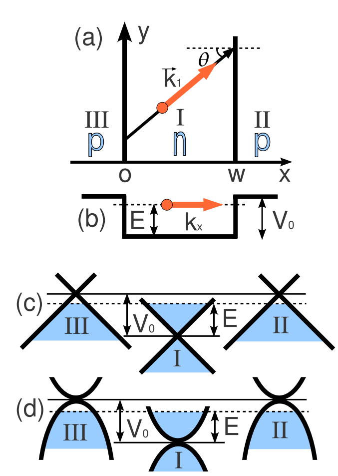


FIG. 1. (Color online) (a) A graphene *p-n-p* waveguide. The width of region I (*n* region) is $w$. A quasiparticle has the momentum $\vec{k}_1$ and the incident angle $\theta=\tan^{-1}(k_y/k_x)$ in the waveguide. (b) Potential diagram of the waveguide. (c) Energy spectrum of the waveguide in SLG. (d) BLG.

 

spinors $\psi=[\psi^A(x,y),\psi^B(x,y)]^T$, where $\psi^A(x,y)$ and $\psi^B(x,y)$ represent the smooth enveloping functions in each sublattice. Therefore, Eq. (1) can be rewritten as

$$-i\hbar v_F\left(\frac{\partial}{\partial x}-i\frac{\partial}{\partial y}\right)\psi^B=(E-V)\psi^A, \tag{3a}$$

$$-i\hbar v_F\left(\frac{\partial}{\partial x}+i\frac{\partial}{\partial y}\right)\psi^A=(E-V)\psi^B. \tag{3b}$$

To solve Eqs. (3), we define $k_1=|E|/\hbar v_F$, $k_2=|E-V_0|/\hbar v_F$, $k_x=k_1\cos\theta$, and $k_y=k_1\sin\theta$, where $\theta$ is the incident angle. Furthermore, the total internal reflection at the *p-n* interfaces requires the condition $V_0/2<E<V_0$ and the critical angle $\sin\theta_c=k_2/k_1$. Due to conservation of $k_y$, we can assume $\psi^m(x,y)=\phi^m(x)e^{ik_y y}$, $m=A, B$ and obtain

$$\psi_{\rm I}=\begin{pmatrix} a\cos(k_x x)+b\sin(k_x x)\\ ia\sin(k_x x+\theta)-ib\cos(k_x x+\theta)\end{pmatrix}e^{ik_y y}, \tag{4a}$$

$$\psi_{\rm II}=c\begin{pmatrix}1\\ -i(\delta+\sin\theta)/\sin\theta_c\end{pmatrix}e^{-\alpha(x-w)+ik_y y}, \tag{4b}$$

$$\psi_{\rm III}=d\begin{pmatrix}1\\ i(\delta-\sin\theta)/\sin\theta_c\end{pmatrix}e^{\alpha x+ik_y y}, \tag{4c}$$

where I, II, and III are the regions shown in Fig. 1, $\delta=(\sin^2\theta-\sin^2\theta_c)^{1/2}$, and $\alpha=(k_y^2-k_2^2)^{1/2}$. The boundary conditions at $x=0$ and $x=w$ lead to a transcendental equation

$$\delta\cos\theta\cos\xi+(\sin\theta_c+\sin^2\theta)\sin\xi=0, \tag{5}$$

where $\xi=k_1 w\cos\theta$. This equation gives the dispersion relations in terms of $E$ and $k_y$ for the guided modes. Numerical calculations of the dispersion relations clearly indicate the slow (forward), zero, and even negative (backward) group velocities of the quasiparticles depending on the gate voltages [Fig. 2(a)] and the widths [Fig. 2(b)].

More interestingly, the voltage-dependent dispersion curves shown in Fig. 2(a) indicate the possibility to dynamically and coherently decelerate, stop, and reaccelerate the guided quasiparticles. The detailed process is as follows. First, we use the fact that the incident angle $\theta$ of the guided quasiparticles is conserved if the interfaces are parallel [Fig. 1(a)]. Thus, assuming the quasiparticles are initially prepared in a forward propagating state shown at point A in Fig. 2(a), then one can adiabatically change the gate voltages to transfer the forward propagating state to a trapped state at point B. After a certain storage time, the trapped state can be transferred to either the original state or a backward propagating state shown at point C. Thus, the *p-n-p* waveguide can function as an electric-field induced coherent "buffer" or "memory" for the guided SLG quasiparticles.

To explain this process, we consider the current densities in the propagation direction, which are

$$J_{y,n}=v_F(\psi_n^\dagger\sigma_y\psi_n), \tag{6}$$

with $n=$I, II, III for the corresponding regions.[30] Hence, the flux $\Phi$, which also gives the group velocity $v_g$ of the quasiparticles, can be given by

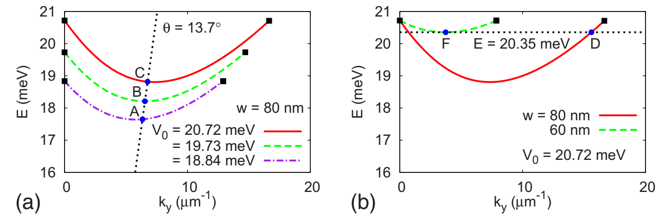


FIG. 2. (Color online) (a) Dispersion curves for the same width of $w=80$ nm, but the different electrostatic potentials: $V_0=20.72$ meV (solid), 19.73 meV (dashed) and 18.84 meV (dash-dotted). For a particular incident angle $\theta=13.7°$ (dotted), one can obtain the different group velocities: 48 279.4 m/s at point A (6.3 $\mu$m$^{-1}$, 17.7 meV), zero at B (6.5 $\mu$m$^{-1}$, 18.2 meV), and −53399.7 m/s at C (6.8 $\mu$m$^{-1}$, 18.8 meV) on the corresponding curves. (b) Dispersion curves for the same electrostatic potential of $V_0=20.72$ meV, but the different widths: $w=80$ nm (solid) and 60 nm (dashed). For a particular incident energy $E=20.35$ meV (dotted), one can obtain the different group velocities: 493 403.4 m/s at point D (15.6 $\mu$m$^{-1}$, 20.35 meV) and zero at F (3.7 $\mu$m$^{-1}$, 20.35 meV) on the corresponding curves. For simplicity, our parameters only lead to one single dispersion curve for each pair of $w$ and $V_0$. The solid black squares give the cutoffs for each case.

$$\Phi=v_g=\int_{-\infty}^{+\infty}(J_{y,\rm I}+J_{y,\rm II}+J_{y,\rm III})dx, \tag{7}$$

where $J_{y,\rm I}$ gives the positive current density in region I for the guided components, and $J_{y,\rm II}$ and $J_{y,\rm III}$ give the negative current densities in regions II and III for the evanescent components. By adiabatically changing the gate voltages, we can coherently redistribute the current densities in the different regions. Thus, the group velocity can be coherently controlled.

Alternatively, the width-dependent dispersion curves shown in Fig. 2(b) also indicate the possibility to coherently decelerate and stop the guided quasiparticles by adiabatically reducing the width from point D to F while keeping the gate voltages unchanged, which is analogous to the photon trapping in the tapered LHH proposed in Ref. 23. After the storage, one can adiabatically change the gate voltages for retrieval.

In a BLG *p-n-p* waveguide [Figs. 1(a), 1(b), and 1(d)], we consider "Bernal stacking" in terms of four sublattices with $A1$, $B1$ in the upper layer and $A2$, $B2$ in the lower layer.[8,14] The BLG Hamiltonian thus reads as[8,14]

$$H=\begin{pmatrix} V & \pi & t_\perp & 0\\ \pi^\dagger & V & 0 & 0\\ t_\perp & 0 & V & \pi^\dagger\\ 0 & 0 & \pi & V\end{pmatrix}, \tag{8}$$

where the interlayer hopping term $t_\perp\approx 400$ meV, $\pi=-i\hbar v_F(\partial/\partial x+i\partial/\partial y)$, $V$ is given by Eq. (2), and $V_0\ll t_\perp$ is assumed for low-energy regime. The eigenstates of Eq. (8) can be written as four-component spinors $\psi=[\psi^{A1},\psi^{B1},\psi^{B2},\psi^{A2}]^T$, where the different components give the different smooth enveloping functions in the correspondingly labeled sublattices.

The quasiparticle dynamics is described by $H\psi=E\psi$, where $E$ is the eigenenergy. In detail, this equation can be rewritten as

$$\pi\psi^{B1}+t_{\perp}\psi^{B2}=(E-V)\psi^{A1}, \tag{9a}$$

$$\pi^{\dagger}\psi^{A1}=(E-V)\psi^{B1}, \tag{9b}$$

$$\pi^{\dagger}\psi^{A2}+t_{\perp}\psi^{A1}=(E-V)\psi^{B2}, \tag{9c}$$

$$\pi\psi^{B2}=(E-V)\psi^{A2}, \tag{9d}$$

where the total internal reflection at the BLG $p$-$n$ interfaces requires $V_0/2<E<V_0$. The spectra for quasiparticles in the different regions are

$$E^2 \pm Et_{\perp}-k_1^2=0, \tag{10}$$

$$(E-V_0)^2 \pm (E-V_0)t_{\perp}-k_2^2=0, \tag{11}$$

where $k_1$ ($k_2$) is the effective total momentum in region I (II and III), and we use $\hbar=v_F=1$ for notational convenience. The translational invariance along the $y$ direction leads to $\psi^m=\phi^m(x)e^{ik_y y}$, $m=A1, B1, A2, B2$. In region I, we can assume[6]

$$\phi_{\rm I}^{B2}=a\cos k_x x+b\sin k_x x+ce^{\alpha x}+de^{-\alpha x}, \tag{12a}$$

$$\phi_{\rm I}^{A2}=i(k_y\phi_{\rm I}^{B2}-\phi_{\rm I}^{B2\prime})/E, \tag{12b}$$

$$\phi_{\rm I}^{A1}=[(E^2+k_y^2)\phi_{\rm I}^{B2}-\phi_{\rm I}^{B2\prime\prime}]/(Et_{\perp}), \tag{12c}$$

$$\phi_{\rm I}^{B1}=i[(E^2+k_y^2)(k_y\phi_{\rm I}^{B2}+\phi_{\rm I}^{B2\prime})-(k_y\phi_{\rm I}^{B2\prime\prime}+\phi_{\rm I}^{B2\prime\prime\prime})]/(E^2t_{\perp}). \tag{12d}$$

In regions II and III, we assume the evanescent waves

$$\phi_{\rm II}^{B2}=fe^{-\beta(x-w)}+ge^{-\gamma(x-w)}, \tag{13}$$

$$\phi_{\rm III}^{B2}=he^{\beta x}+le^{\gamma x}, \tag{14}$$

and other components are similar to those in region I except that $E-V_0$ replaces $E$. In Eqs. (12a)–(12d), (13), and (14), [ $'$ ] represents $d/dx$, $k_x=(E^2+Et_{\perp}-k_y^2)^{1/2}$, $\alpha=(k_y^2-E^2+Et_{\perp})^{1/2}$, $\beta=(k_y^2-\tilde{E}^2+\tilde{E}t_{\perp})^{1/2}$, $\gamma=(k_y^2-\tilde{E}^2-\tilde{E}t_{\perp})^{1/2}$, and $\tilde{E}=E-V_0$. The boundary conditions at $x=0$ and $x=w$ lead to an $8\times 8$ coefficient determinant and then yield a transcendental equation. This equation gives the dispersion relations between $E$ and $k_y$ in the BLG $p$-$n$-$p$ waveguide. The equation is not analytically shown here due to its complexity, but the numerical results shown in Fig. 3 give the slow, zero, and negative group velocities of the guided BLG quasiparticles. Also, the aforementioned methods in the SLG waveguide are applicable to coherently control the guided BLG quasiparticles.

Again, we consider the $y$ components of current densities in the different regions

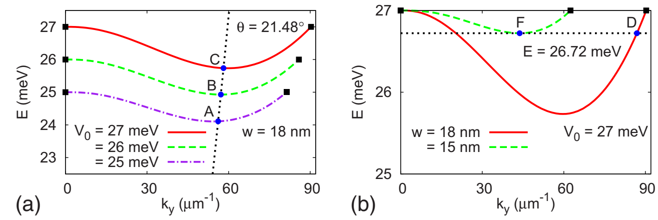


FIG. 3. (Color online) (a) Dispersion curves for the same width $w=18$ nm, but the different electrostatic potentials: $V_0=27$ meV (solid), 26 meV (dashed), and 25 meV (dash-dotted). For a particular incident angle $\theta=21.48°$ (dotted), the different group velocities can be obtained: 5252.7 m/s at point A (56.1 $\mu$m$^{-1}$, 24.1 meV), zero at B (57.1 $\mu$m$^{-1}$, 24.9 meV), and −5311.0 m/s at C (58.1 $\mu$m$^{-1}$, 25.7 meV) on the corresponding curves. (b) Dispersion curves for the same electrostatic potential $V_0=27$ meV but the different widths: $w=18$ nm (solid) and 15 nm (dashed). For a particular incident energy $E=26.72$ meV (dotted), the different group velocities can be obtained: 115 180.5 m/s at point D (86.9 $\mu$m$^{-1}$, 26.72 meV) and zero at F (43.7 $\mu$m$^{-1}$, 26.72 meV) on the corresponding curves. For simplicity, our parameters only lead to one single dispersion curve for each pair of $w$ and $V_0$. The solid black squares give the cutoffs for each case.

$$J_{y,n}=v_F\left(\psi_n^{\dagger}\begin{pmatrix}\sigma_y & 0\\ 0 & \sigma_y\end{pmatrix}\psi_n\right), \tag{15}$$

with $n$=I, I, III for the corresponding regions.[31] Similar to Eq. (7), we can calculate the flux $\Phi$ and the group velocity $v_g$ of the guided BLG quasiparticles.

Based on our results, it is clearly seen that, the interband tunneling through the $p$-$n$ interfaces in graphene waveguides plays an essential role in group-velocity control for both SLG (massless) and BLG (massive) quasiparticles. This tunneling can produce opposite current densities in the adjacent regions and thus affect the propagation of the entire wave functions of the guided modes. In addition, *trilayer* graphene (TLG) has recently attracted great attention.[32,33] Notice that interband tunneling can also occur through TLG $p$-$n$ interfaces. Therefore, our scheme might be extended to coherently control quasiparticles in TLG $p$-$n$-$p$ waveguides.

In summary, we have shown the interesting dispersion relations in both SLG and BLG $p$-$n$-$p$ waveguides due to the interband tunneling through the $p$-$n$ interfaces. By adiabatically changing some parameters (e.g., the gate voltages and the widths), it is possible to coherently decelerate, stop, and reaccelerate the guided graphene quasiparticles in waveguides. Hence, graphene $p$-$n$-$p$ waveguides offer multiple functionalities (i.e., waveguiding, buffering, and trapping) for coherent manipulation of quasiparticles in both SLG and BLG. Our findings may simplify the use and fabrication of graphene-based integrated coherent devices.

We would like to acknowledge funding from NSF. L.Z. thanks J. Javanainen, W. Duan, R. Zhou, T. Wang, and F. Peng for helpful discussions.

[1] K. S. Novoselov, A. K. Geim, S. V. Morozov, D. Jiang, Y. Zhang, S. V. Dubonos, I. V. Grigorieva, and A. A. Firsov, Science **306**, 666 (2004).
[2] A. H. Castro Neto, F. Guinea, N. M. Peres, K. S. Novoselov, and A. K. Geim, Rev. Mod. Phys. **81**, 109 (2009).
[3] C. W. J. Beenakker, Rev. Mod. Phys. **80**, 1337 (2008).
[4] K. S. Novoselov, A. K. Geim, S. V. Morozov, D. Jiang, M. I. Katsnelson, I. V. Grigorieva, S. V. Dubonos, and A. A. Firsov, Nature (London) **438**, 197 (2005).
[5] Y. Zhang, Y. W. Tan, H. L. Stormer, and P. Kim, Nature (London) **438**, 201 (2005).
[6] M. I. Katsnelson, K. S. Novoselov, and A. K. Geim, Nat. Phys. **2**, 620 (2006).
[7] K. S. Novoselov, E. McCann, S. V. Morozov, V. I. Fal'ko, M. I. Katsnelson, U. Zeitler, D. Jiang, F. Schedin, and A. K. Geim, Nat. Phys. **2**, 177 (2006).
[8] E. McCann and V. I. Fal'ko, Phys. Rev. Lett. **96**, 086805 (2006).
[9] J. B. Oostinga, H. B. Heersche, X. Liu, A. F. Morpurgo, and L. M. K. Vandersypen, Nature Mater. **7**, 151 (2008).
[10] S. Datta, *Electronic Transport in Mesoscopic Systems* (Cambridge University Press, Cambridge, England, 1995).
[11] P. G. Silvestrov and K. B. Efetov, Phys. Rev. Lett. **98**, 016802 (2007).
[12] B. Trauzettel, D. V. Bulaev, D. Loss, and G. Burkard, Nat. Phys. **3**, 192 (2007).
[13] A. Matulis and F. M. Peeters, Phys. Rev. B **77**, 115423 (2008).
[14] J. Milton Pereira, Jr., P. Vasilopoulos, and F. M. Peeters, Nano Lett. **7**, 946 (2007).
[15] A. De Martino, L. Dell'Anna, and R. Egger, Phys. Rev. Lett. **98**, 066802 (2007).
[16] L. Oroszlany, P. Rakyta, A. Kormanyos, C. J. Lambert, and J. Cserti, Phys. Rev. B **77**, 081403(R) (2008).
[17] M. Ramezani Masir, P. Vasilopoulos, A. Matulis, and F. M. Peeters, Phys. Rev. B **77**, 235443 (2008).
[18] A. Kormányos, P. Rakyta, L. Oroszlány, and J. Cserti, Phys. Rev. B **78**, 045430 (2008).
[19] M. Ramezani Masir, A. Matulis, and F. M. Peeters, Phys. Rev. B **79**, 155451 (2009).
[20] C. H. Park, Y. W. Son, L. Yang, M. L. Cohen, and S. G. Louie, Nano Lett. **8**, 2920 (2008).
[21] P. Darancet, V. Olevano, and D. Mayou, Phys. Rev. Lett. **102**, 136803 (2009).
[22] V. V. Cheianov, V. Fal'ko, and B. L. Altshuler, Science **315**, 1252 (2007).
[23] K. L. Tsakmakidis, A. D. Boardman, and O. Hess, Nature (London) **450**, 397 (2007).
[24] C. W. J. Beenakker, R. A. Sepkhanov, A. R. Akhmerov, and J. Tworzydło, Phys. Rev. Lett. **102**, 146804 (2009).
[25] F. Zhang, Y. He, and X. Chen, Appl. Phys. Lett. **94**, 212105 (2009).
[26] K. S. Kim, Y. Zhao, S. Y. Lee, J. M. Kim, K. S. Kim, J.-H. Ahn, P. Kim, J.-Y. Choi, and B. H. Hong, Nature (London) **457**, 706 (2009).
[27] X. Li, W. Cai, J. An, S. Kim, J. Nah, D. Yang, R. Piner, A. Velamakanni, I. Jung, E. Tutuc, S. K. Banerjee, L. Colombo, and R. S. Ruoff, Science **324**, 1312 (2009).
[28] B. Huard, J. A. Sulpizio, N. Stander, K. Todd, B. Yang, and D. Goldhaber-Gordon, Phys. Rev. Lett. **98**, 236803 (2007).
[29] A. F. Young and P. Kim, Nat. Phys. **5**, 222 (2009).
[30] J. M. Pereira, Jr., V. Mlinar, F. M. Peeters, and P. Vasilopoulos, Phys. Rev. B **74**, 045424 (2006).
[31] I. Snyman and C. W. J. Beenakker, Phys. Rev. B **75**, 045322 (2007).
[32] F. Guinea, A. H. Castro Neto, and N. M. R. Peres, Phys. Rev. B **73**, 245426 (2006).
[33] M. F. Craciun, S. Russo, M. Yamamoto, J. B. Oostinga, A. F. Morpurgo, and S. Tarucha, Nat. Nanotechnol. **4**, 383 (2009).